Crystal structure of *Mycobacterium tuberculosis* ClpP1P2 suggests a model for peptidase activation by AAA+ partner binding and substrate delivery

Karl R. Schmitz[a], Daniel W. Carney[b], Jason K. Sello[b], and Robert T. Sauer[a,1]

[a]Department of Biology, Massachusetts Institute of Technology, Cambridge, MA 02139; and [b]Department of Chemistry, Brown University, Providence, RI 02912

Contributed by Robert T. Sauer, September 4, 2014 (sent for review August 8, 2014)

Caseinolytic peptidase P (ClpP), a double-ring peptidase with 14 subunits, collaborates with ATPases associated with diverse activities (AAA+) partners to execute ATP-dependent protein degradation. Although many ClpP enzymes self-assemble into catalytically active homo-tetradecamers able to cleave small peptides, the *Mycobacterium tuberculosis* enzyme consists of discrete ClpP1 and ClpP2 heptamers that require a AAA+ partner and protein–substrate delivery or a peptide agonist to stabilize assembly of the active tetradecamer. Here, we show that cyclic acyldepsipeptides (ADEPs) and agonist peptides synergistically activate ClpP1P2 by mimicking AAA+ partners and substrates, respectively, and determine the structure of the activated complex. Our studies establish the basis of heteromeric ClpP1P2 assembly and function, reveal tight coupling between the conformations of each ring, show that ADEPs bind only to one ring but appear to open the axial pores of both rings, provide a foundation for rational drug development, and suggest strategies for studying the roles of individual ClpP1 and ClpP2 rings in Clp-family proteolysis.

AAA+ proteases | allosteric coupling | pathogen drug target

The self-compartmentalized caseinolytic peptidase P (ClpP) functions in collaboration with the ATPases associated with diverse activities (AAA+) ClpX, ClpA, or ClpC enzymes to carry out ATP-dependent proteolysis in bacteria and eukaryotic organelles (1). The physiological importance of these proteolytic complexes is reflected in their requirement for the viability and/or virulence of some bacteria and the observation that loss-of-function mutations in mammals are linked to developmental defects and disease (2–8). Most well-characterized ClpP enzymes come from organisms that have a single *clpP* gene and consist of identical heptameric rings, which stack face-to-face to enclose a degradation chamber in which 14 active sites mediate peptide-bond hydrolysis (1, 9, 10). Importantly, the proteolytic chamber is accessible only via narrow axial pores that allow entry of small peptides, greatly slow entry of larger peptides or unfolded proteins, and block access of native proteins (11, 12). Degradation of proteins is mediated by the ClpXP, ClpAP, or ClpCP proteolytic complexes. In these enzymes, the AAA+ partner forms a ring hexamer that binds peptide degrons in target proteins, unfolds native structure if necessary, and translocates the unfolded polypeptide through a central channel and into the lumen of ClpP for degradation (13).

When AAA+ partner proteins bind to ClpP, one consequence is opening of the narrow axial pores (12, 14, 15). Binding is mediated in part by tripeptide motifs [typically Ile-Gly-Phe or Leu-Gly-Phe (LGF)] in flexible loops in the AAA+ hexamer, which dock into hydrophobic pockets at subunit interfaces on each ClpP heptamer (16–19). In a remarkable example of protein mimicry by a natural product, cyclic acyldepsipeptide (ADEP) antibiotics bind in the same hydrophobic pockets on ClpP and also open the axial pores, potentially leading to unregulated protein degradation and cell death (14, 15, 20, 21).

In contrast to organisms with one ClpP, two or more ClpP isoforms are characteristic of two large bacterial phyla (Actinobacteria and Cyanobacteria) and also occur in individual species from other phyla (22, 23). For example, *Mycobacterium tuberculosis,* a pathogenic actinobacterium, encodes cotranscribed *clpP1* and *clpP2* genes (24, 25). The importance of Clp-family proteolysis in *M. tuberculosis* is highlighted by the facts that the *clpP1*, *clpP2*, *clpX*, and *clpC1* genes are all essential and that mechanism-based ClpP inhibitors suppress growth (24, 26–28). Recent studies indicate that *M. tuberculosis* ClpP1 and ClpP2 form discrete heptameric rings that assemble into an active ClpP1P2 tetradecamer only in the presence of a ClpX or ClpC1 AAA+ partner and one additional factor, either protein substrates being actively translocated into the degradation chamber or N-blocked peptide agonists (23, 29). Because *M. tuberculosis* resistance to conventional antibacterial drugs is a major health hazard, there is substantial interest in developing drugs that target ClpP1P2. At the outset of this work, however, there was no structure of *M. tuberculosis* ClpP1P2 or any heteromeric ClpP enzyme to guide design efforts.

Here, we show that a catalytically active ClpP1P2 tetradecamer can be stabilized by the combination of a novel ADEP and an agonist peptide, which allowed crystallization and determination of the 3D structure. Together, our structural and biochemical results reveal the basis for ClpP1P2 assembly and activation, establish that the conformations of the ClpP1 and ClpP2 rings are tightly coupled, show that ADEPs bind exclusively to one ring, and suggest strategies for the design of active ClpP1 or ClpP2 tetradecamers for studies of AAA+ partner specificity and biological function.

Significance

Caseinolytic peptidase P (ClpP) normally collaborates with ATPases associated with diverse activities (AAA+) partner proteins, such as ClpX and ClpC, to carry out energy-dependent degradation of proteins within cells. The ClpP enzyme from *Mycobacterium tuberculosis* is required for survival of this human pathogen, is a validated drug target, and is unusual in consisting of discrete ClpP1 and ClpP2 rings. We solved the crystal structure of ClpP1P2 bound to peptides that mimic binding of protein substrates and small molecules that mimic binding of a AAA+ partner and cause unregulated rogue proteolysis. These studies explain why two different ClpP rings are required for peptidase activity and provide a foundation for the rational development of drugs that target ClpP1P2 and kill *M. tuberculosis*.

Author contributions: K.R.S., D.W.C., J.K.S., and R.T.S. designed research; K.R.S. and D.W.C. performed research; D.W.C. contributed new reagents/analytic tools; K.R.S. analyzed data; and K.R.S., D.W.C., J.K.S., and R.T.S. wrote the paper.

The authors declare no conflict of interest.

Data deposition: Crystallography, atomic coordinates, and structure factors reported in this paper have been deposited in the Protein Data Bank, www.pdb.org (PDB ID codes 4U0G and 4U0H).

[1]To whom correspondence should be addressed. Email: bobsauer@mit.edu.

This article contains supporting information online at www.pnas.org/lookup/suppl/doi:10.1073/pnas.1417120111/-/DCSupplemental.

Results

ADEPs Activate *M. tuberculosis* ClpP1P2 and Block ClpX Binding in Vitro. ADEPs bind to many homomeric ClpP enzymes and activate cleavage of large peptides and unstructured proteins (20, 21). They also inhibit *M. tuberculosis* growth in the presence of efflux-pump inhibitors (30), strongly suggesting that ClpP1P2 also should be an ADEP target, with toxicity resulting either from activation of rogue degradation and/or from inhibition of interaction with a AAA+ partner. To test for activation, we assayed ClpP1P2 cleavage of a decapeptide in the presence of known and novel ADEP analogs having macrocycles of differing rigidity and either straight or branched acyl side chains (Fig. 1*A*) (30, 31). We found that ClpP1P2 was activated in the presence of both an ADEP and a peptide agonist [in this experiment carboxybenzyl-leucine-leucine-norvaline-aldehyde (Z-Leu-Leu-Nva-CHO)], a combination that did not activate cleavage by ClpP1 alone or ClpP2 alone (Fig. 1*B*). In titration studies, ClpP1P2 activation displayed positive cooperativity with half-maximal ADEP stimulatory concentrations from ~5 to >250 μM depending on the molecule (Fig. 1*C* and Table S1). The tighter-binding ADEPs had a more rigid macrocycle, as anticipated from previous ClpP-activation studies (30, 31). Methyl branching on the acyl side chain was important also. Indeed, ADEP-2B^{5Me} and ADEP-2B^{6Me}, two of the tightest binders, had acyl side chains reminiscent of Ile and Leu, which are the most common residues at the first position of the AAA+ tripeptide-docking motif (16). The ADEPs tested also had a difluorophenylalanine that mimics the last residue in the tripeptide motif (15), which is LGF in *M. tuberculosis* ClpX and ClpC1.

To assess how different combinations of ADEP and a Z-Ile-Leu agonist peptide affected the reactivity of the peptidase active sites, we used a fluorescent reagent, tetramethylrhodamine (TAMRA)-fluorophosphonate, that modifies active-site serines and a ClpP1P2 variant in which ClpP1 was fused to a C-terminal small ubiquitin-related modifier (SUMO) domain to allow separation from ClpP2 by SDS/PAGE. Following incubation for different time periods, samples were run on a gel, and active-site reactivity was assessed by fluorescence (Fig. 1*D*). In these experiments, ADEP-2B alone increased the rate of active-site modification of ClpP2 modestly, Z-Ile-Leu alone had little effect on active-site reactivity, but the combination of ADEP-2B and Z-Ile-Leu increased the rate of modification of both ClpP1 and ClpP2 substantially. These results in combination with the activation results described above indicate that ADEPs and agonist peptides bind to an enzymatically active conformation of ClpP1P2 and, in

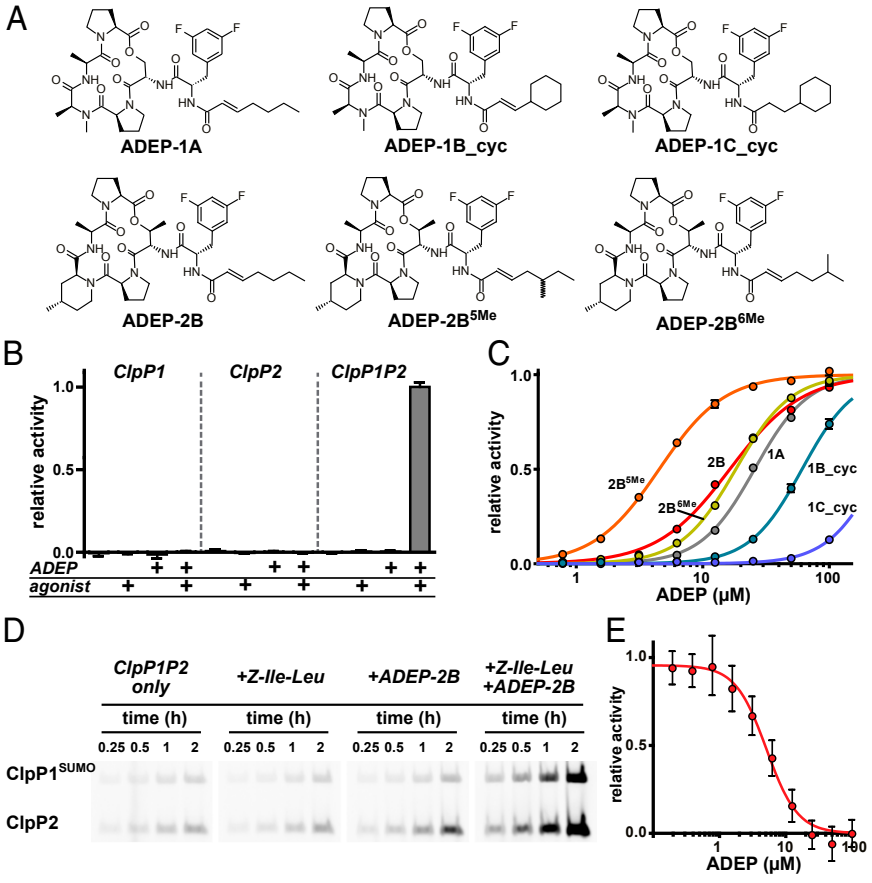

Fig. 1. ADEPs activate *M. tuberculosis* ClpP1P2 in vitro. (*A*) Chemical structures of ADEPs used in this study. The syntheses of ADEP-1A, ADEP-1B_cyc, ADEP-1C_cyc (IRD-10011), and ADEP-2B have been described (30, 31, 37). The synthesis of ADEP-2B^{5Me} and ADEP-2B^{6Me} are described in *SI Methods*. (*B*) Cleavage of a fluorogenic decapeptide (15 μM) by ClpP1 alone (0.25 μM), ClpP2 alone (0.25 μM), or ClpP1 and ClpP2 (0.25 μM each) was assayed in the absence or presence of Z-Leu-Leu-Nva-CHO agonist (50 μM) and/or ADEP-2B (20 μM). Robust peptidase activity required ClpP1, ClpP2, agonist, and ADEP. (*C*) Cleavage of the decapeptide peptide substrate (15 μM) by ClpP1P2 (0.25 μM) was assayed in the presence of increasing concentrations of different ADEPs and Z-Leu-Leu-Nva-CHO agonist (50 μM). Values are averages ± SD (n = 3); many error bars are smaller than the plot symbols. Data were fit to a Hill equation (fitted parameters are listed in Table S1). (*D*) A complex consisting of ClpP1^{SUMO} and ClpP2 (0.25 μM each) was incubated with TAMRA-fluorophosphonate (2 μM) for different times in the absence or presence of Z-Ile-Leu peptide (0.5 mM) and/or ADEP-2B (50 μM). Samples were denatured and electrophoresed on SDS gels, and TAMRA fluorescence was detected using a fluorescence imager. (*E*) Increasing concentrations of ADEP-2B inhibited degradation of GFP-ssrA (10 μM) by ClpX (0.5 μM) and ClpP1P2 (2 μM). Values are averages ± SD (n = 3). The line is a fit to a Hill equation; fitted parameters are listed in Table S2.

combination, stabilize this structure to a far greater extent than either single ligand alone.

To test the possibility that ADEPs could be toxic because they prevent binding of a AAA+ partner to ClpP1P2, we assayed degradation of a degron-tagged protein substrate (GFP-ssrA) by *M. tuberculosis* ClpX and ClpP1P2 in the presence of increasing concentrations of ADEP-2B (Fig. 1*E*). Strikingly, complete inhibition of GFP-ssrA degradation was observed at high ADEP concentrations, supporting a model in which ADEP binding to ClpP1P2 blocks ClpX binding. These results also show that ADEP-activated ClpP1P2 cannot degrade the natively folded protein substrate used in this experiment.

Crystal Structures. Crystals grew over the course of ~9 mo in drops containing selenomethionine-labeled ClpP1, native ClpP2, ADEP-2B^{5Me}, and a Z-Ile-Leu agonist peptide. Diffraction data to ~3.2-Å resolution were collected on two crystals with different morphologies from a single crystallization drop, and the structures were solved by molecular replacement (Table 1). One crystal form had two ClpP1P2 tetradecamers in the asymmetric unit. Despite the modest resolution, the use of noncrystallographic symmetry during refinement (14 copies of each chain in the asymmetric unit) resulted in clear electron-density maps (Fig. 2*A* and Fig. S1), R and R_{free} values of ~0.19 and ~0.22, respectively, and good model geometry (Table 1). Both the distribution of selenium sites in an anomalous map from the initial molecular replacement solution (Fig. S2) and structural refinement established that each tetradecamer consisted of one heptameric ring of selenomethionine-labeled ClpP1 and one heptameric ring of unlabeled ClpP2 (Fig. 2*B*). The two ClpP1P2 tetradecamers in the asymmetric unit had similar structures. The individual heptameric ClpP1 and ClpP2 rings in ClpP1P2 had similar overall conformations, with an rmsd of 0.72 Å for common main-chain atoms. The equatorial interface between the ClpP1 and ClpP2 rings was well ordered (Fig. 2*A*), and the heteromeric complex adopted an extended conformation (~93 Å high; ~96 Å across; Fig. 2 *B–D*), similar to the active conformations of homomeric tetradecamers of other bacterial ClpP peptidases (1). The second crystal contained a ClpP1P1 tetradecamer (Fig. 2 *E* and *F*), which was shorter and wider than the ClpP1P2 tetradecamer (Fig. 2 *B* and *E*) and was nearly identical to a previous structure (32) with respect to all-atom rmsd (0.32 Å), space group, and unit-cell dimensions (Table 1).

Table 1. Data collection and refinement statistics (molecular replacement)

Parameters	ClpP1P2•ADEP•Z-Ile-Leu (PDB ID code 4U0G)	ClpP1 (PDB ID code 4U0H)
Data collection		
Space group	$P2_12_12_1$	$P6_122$
Cell dimensions		
a, *b*, *c*, Å	154.8, 187.6, 294.0	178.9, 178.9, 265.3
α, β, γ, °	90, 90, 90	90, 90, 120
Resolution, Å	50 (3.20)	50 (3.25)
R_{sym}	0.152 (0.550)	0.192 (0.514)
Average I/σI	13.5 (3.6)	12.8 (5.1)
Completeness, %	100 (100)	98.9 (98.7)
Redundancy	6.8 (7.1)	6.0 (6.3)
Refinement		
Resolution, Å	3.20	3.25
No. reflections	140,896	39,709
R_{work}/R_{free}	0.190/0.222	0.180/0.214
No. nonhydrogen atoms		
Protein	39,266	9,426
ADEP-2B^{5Me}	798	—
Z-Ile-Leu	756	—
Other ligands	235	70
Water	29	34
β-Factors		
Protein	33.2	26.5
ADEP-2B^{5Me}	45.0	—
Z-Ile-Leu	59.2	—
Other ligands	58.2	79.6
Water	15.2	12.8
rmsd		
Bond lengths, Å	0.004	0.003
Bond angles, °	0.705	0.631

Data were collected on a single crystal for each structure. Values in parentheses represent the highest-resolution shell.

In the ClpP1P2 tetradecamer, ADEP-2B^{5Me} molecules were bound exclusively in the LGF-binding pockets of ClpP2, whereas Z-Ile-Leu agonist peptides were bound within all 14 active sites (Fig. 2 *B–D*). Although the ClpP1P1 crystals grew in the presence of ADEP-2B^{5Me} and Z-Ile-Leu, neither ligand was bound in the structure. In the ClpP1P2 structure, the dimensions of the axial pore of the ClpP1 ring (~30 Å wide) and ClpP2 ring (~25 Å wide) were substantially larger than the axial pores of the ClpP1 rings in the ClpP1P1 complex (~12 Å), although disordered residues may fill some of the pore in each of these structures (Fig. 2 *C*, *D*, and *F*).

As described in detail below, the binding of ADEP-2B^{5Me} to the LGF-pockets of ClpP2, the binding of peptide agonists within the active sites of ClpP2 and ClpP1, the active-site architecture, and the overall structure of ClpP1P2 were all indicative of a catalytically competent conformation. The well-structured equatorial interface in ClpP1P2 also is a feature observed in the active conformations of homomeric ClpP enzymes (1), although the latter structures have a symmetric equatorial interface, whereas the interface in ClpP1P2 was asymmetric. Conversely, the symmetric equatorial interface in the compressed ClpP1P1 tetradecamer was somewhat disordered, and the active-site architecture and absence of agonist peptides were consistent with an inactive conformation. Indeed, modeling Z-Ile-Leu in the conformation observed in the ClpP1-active sites of ClpP1P2 into the ClpP1P1 structure predicted major steric clashes with main-chain and side-chain atoms.

Exclusive Binding of ADEP to ClpP2. ADEP-2B^{5Me} occupied the LGF-binding pockets at each subunit–subunit interface in the ClpP2 ring (Fig. 2*C* and Fig. S3*A*) and bound largely as in other ADEP•ClpP structures (14, 15). The Ile-like acyl portion of ADEP-2B^{5Me} filled a groove lined by hydrophobic residues and the aliphatic portions of the Lys35 and Glu39 side chains of ClpP2, whereas the difluorophenylalanine ring projected snuggly into a triangular hydrophobic pocket with a narrow opening (Fig. 3 *A–C* and Fig. S3*A*). As noted above, these interactions likely partially mimic contacts made by LGF peptides in flexible loops of *M. tuberculosis* ClpX and/or ClpC1. The acyl and difluorophenylalanine parts of ADEP-2B^{5Me} made predominantly hydrophobic interactions with ClpP2, whereas the macrocycle made numerous polar and apolar contacts that appear to be stabilized by transannular hydrogen bonds that constrain its conformation (Fig. 3*A*).

The presence of ADEP in only the ClpP2 ring suggests that binding to one ring is sufficient to stabilize an active conformation of both rings. In support of this model, we found that ADEP-2B stimulated the peptidase activity of a complex of wild-type ClpP1 and catalytically inactive ClpP2^{S110A} (Fig. S4). This allosteric effect is in line with the observation that ADEP-2B stimulates fluorophosphonate modification of both active sites (Fig. 1*D*). Higher concentrations of ADEP-2B were needed to activate ClpP1P2^{S110A} than to activate ClpP1P2, and no activation was observed in ClpP1^{S98A}P2, which has an inactivating catalytic mutation in ClpP1 (Fig. S4). These observations suggest that the catalytic

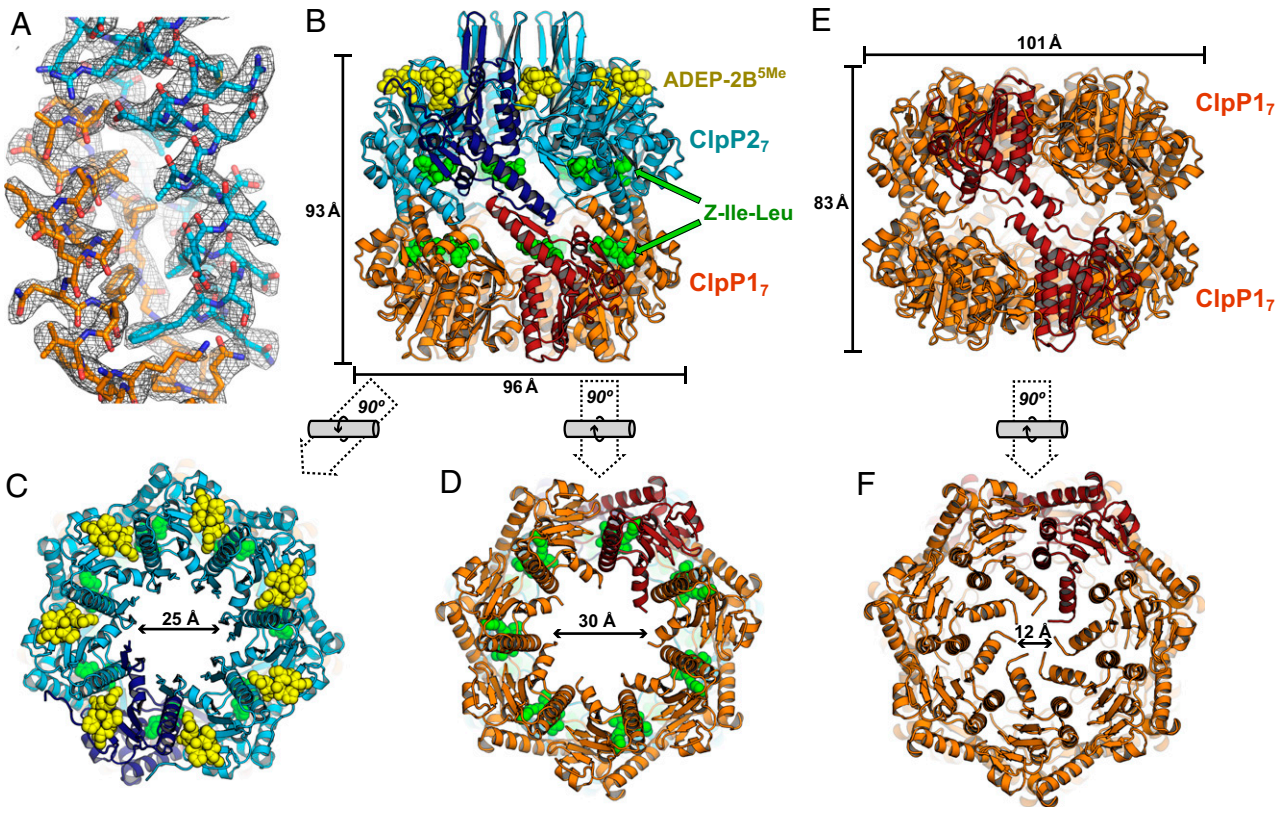

Fig. 2. ClpP1P2 and ClpP1P1 structures. (*A*) Electron-density map (contoured at 1.5 σ) from the ClpP1P2 structure, showing equatorial interactions between residues 124–148 in a ClpP1 subunit (stick representation; orange carbons) and residues 136–162 in a ClpP2 subunit (stick representation; cyan carbons). (*B*) Side view of the ClpP1P2 tetradecamer. The ClpP1 heptamer (orange or red subunits) and ClpP2 heptamer (cyan or blue subunits) are shown in cartoon representation. Spheres represent ADEP-2B^{5Me} molecules (yellow) bound to the ClpP2 ring and Z-Ile-Leu peptides (green) bound to the active sites of both rings. (*C*) Axial view of the ClpP1P2 tetradecamer from the ClpP2 side. (*D*) Axial view of the ClpP1P2 tetradecamer from the ClpP1 side. (*E*) Side view of the ClpP1P1 tetradecamer, which crystallized under the same conditions as ClpP1P2 but did not bind ADEP or Z-Ile-Leu ligands. Note that the structure is wider but shorter than ClpP1P2 (compare with *B*). (*F*) Axial view of the ClpP1P1 tetradecamer. The structural representations and color schemes used in *B* are also used in *C*–*F*.

serine mutations may destabilize active complexes either directly or indirectly by weakening agonist binding (see below).

Modeling suggested that ADEP does not bind to ClpP1 in ClpP1P2 because the macrocycle would clash with the ring of Tyr91, which adopts a rotamer conformation constrained by stacking interactions with flanking aromatic side chains (Fig. S3 *B* and *C*). The pockets for the acyl and difluorophenylalanine parts of the ADEP side chain were present in the ClpP1 ring of ClpP1P2 (Fig. S3*B*) but were eliminated by conformational rearrangements in the compressed and inactive ClpP1P1 structure, suggesting that an ADEP side chain might bind to an active ClpP1 ring. Thus, we tested ClpP1P2 activation by an ADEP-2B fragment (*N*-E-2-heptenoyldifluorophenylalanine methyl ester) in which the side chain was appended to a small methoxy group rather than the bulky macrocycle; this fragment activates *Bacillus subtilis* ClpP and has antibacterial activity (33). In experiments performed in the presence of Z-Ile-Leu agonist, the fragment activated peptide cleavage by ClpP1P2, albeit more weakly and to a lower maximal level than ADEP-2B (Fig. 3*D*). Importantly, however, titration of an equimolar mixture of the fragment and ADEP-2B increased ClpP1P2 activity to a higher maximal level than ADEP alone (Fig. 3*D*), an outcome that would not be expected if both molecules bound only to the ClpP2 ring. Titration of ADEP-2B in the presence of a saturating amount of fragment (200 μM) resulted in a tighter apparent ADEP-2B affinity (Fig. 3*D*), supporting a model in which active ClpP1P2 can be synergistically stabilized by the binding of the fragment to ClpP1 and the binding of ADEP-2B to ClpP2.

ADEP Stabilizes Open-Pore Conformations of ClpP2 Directly and of ClpP1 Indirectly. The N-terminal loops of ClpP2 (N-loops; residues 19–30) formed an extended annulus of β-hairpins projecting ~12 Å above the open ClpP2 pore (Fig. 2*B*). The N-loops of ADEP-bound *Escherichia coli* ClpP project a shorter distance (15), have a more polar sequence at their apex, and interact with pore-2 loops from ClpX, helping mediate productive collaboration during protein degradation (19). These N-loop differences may explain why *E. coli* ClpP does not function with *M. tuberculosis* ClpX or ClpC1 (23).

Glu21 and Lys28 in the ClpP2 β-hairpin form salt bridges with Lys35 and Glu38 in helix α1 of the same subunit (Fig. 4). These interactions and Lys35•••Glu39 and Lys35•••Glu38 salt bridges link the conformation of the N-loops to packing interactions between the Ile-like portion of the ADEP acyl side chain and the nonpolar portions of the Lys35 and Glu39 side chains (Fig. 4), directly stabilizing the open axial pore of the ClpP2 ring. The ClpP2 N-loop conformation also was stabilized in the crystal by interdigitation of N-loops from a ClpP2 ring related by crystallographic symmetry (Fig. S5), which may mimic contacts normally formed by pore-2 loops from a ClpX or ClpC1 AAA+ partner. However, no stabilizing interactions were found between the extended β-hairpins of adjacent N-loops from the same ClpP2 ring, and thus the distal portions of these loops are likely to be conformationally dynamic in the absence of crystal contacts.

The pore of the ClpP1 ring in ClpP1P2 appeared to be open, and the ClpP1 N-loops were disordered (Fig. 2*D*). We cannot exclude the possibility that the ClpP1 pore is closed by multiple

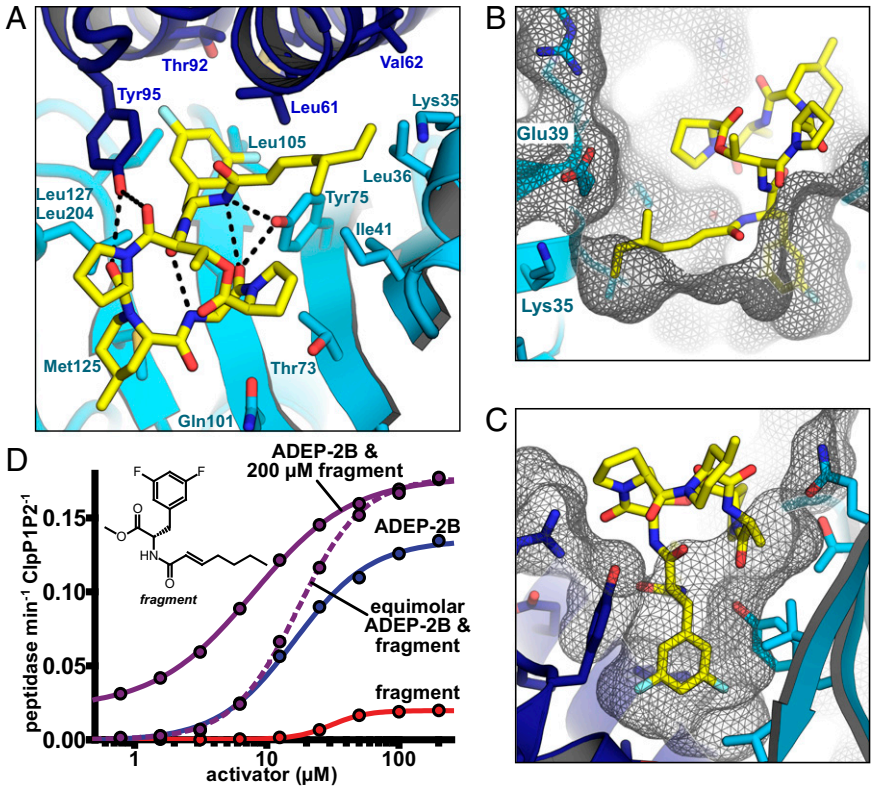

Fig. 3. ADEP binding to ClpP2. (*A*) ADEP-2B^{5Me} (stick representation; yellow carbons) binds in a pocket between adjacent ClpP2 subunits (ribbon representation; one subunit is blue, and one is cyan). Selected side chains of ClpP2 are shown in stick representation. Dashed lines represent hydrogen bonds. The ADEP difluorophenylalanine side chain packs against Leu61, Tyr75, Tyr95, Leu105, and Leu127; the ADEP acyl side chain packs against Leu36, Ile41, Leu61, Tyr75, and the aliphatic portions of Lys35 and Glu39; and the ADEP macrocycle makes hydrophobic interactions with Val103, Met125, and Leu204 and hydrogen bonds with Tyr75, Tyr95, and Arg97. (*B*) The acyl side chain of ADEP-2B^{5Me} lies in a hydrophobic groove on the surface of the ClpP2 ring. (*C*) The difluorophenylalanine side chain of ADEP-2B^{5Me} projects into a deep hydrophobic pocket in the ClpP2 ring. (*D*) V_{max} for ClpP1P2 decapeptide cleavage was 0.02 peptide·min^{-1}·ClpP1P2^{-1} in the presence of saturating ADEP-2B side-chain fragment (*N*-E-2-heptenoyldifluorophenylalanine methyl ester; structure shown; red curve), 0.13 peptide·min^{-1}·ClpP1P2^{-1} for ADEP-2B (blue curve), and 0.18 peptide·min^{-1}·ClpP1P2^{-1} for an equimolar mixture of ADEP-2B and fragment (dashed purple curve). ADEP-2B binding in the presence of the 200-μM fragment (solid purple curve) was tighter (K_{app} = 7.9 ± 0.2 μM) and less cooperative (Hill constant = 1.2 ± 0.03) than in its absence (K_{app} = 16 ± 0.04 μM; Hill constant = 1.5 ± 0.05). In addition to ADEP and/or fragment, reactions contained ClpP1 and ClpP2 (0.25 μM each), decapeptide (15 μM), and Z-Leu-Leu-Nva-CHO peptide (50 μM). Values are averages ± SD (n = 3). Lines are fits to a Hill equation; fitted parameters are listed in Table S1.

conformations of the missing residues, but the "open" pore was clearly very different from the closed pore of the ClpP1P1 structure. We note that the sequences of the N-loops of ClpP1 would not allow them to make some interactions that stabilize the N-loop hairpin of ClpP2 and that the ClpP1 pores face large solvent cavities in both the ClpP1P2 and ClpP1P1 crystals (Fig. S5 *C* and *D*). Thus, it seems unlikely that crystal packing disrupts ordered N-loops around the ClpP1 pore. Given that ADEPs bound only to ClpP2 stabilize an active ClpP1 ring (Fig. 1*D* and Fig. S4), allosteric effects also may stabilize an open-pore conformation of the ClpP1 ring.

Similarities and Differences Between the ClpP1 and ClpP2 Active Sites. In each subunit of both the ClpP1 and ClpP2 rings, the Ser-His-Asp catalytic triad and oxyanion hole adopted a catalytically competent conformation (Fig. 5). Z-Ile-Leu peptides also were present in each active site of both rings of ClpP1P2. However, these agonist peptides bound in the reverse orientation from bona fide peptide substrates, which would pair in an antiparallel manner with the β9 strand (34). In contrast, Z-Ile-Leu paired with this strand in a parallel fashion, with the N-terminal carboxybenzyl-protecting group (indicated by the Z) occupying the S1 substrate-binding pocket (Fig. 5 and Fig. S6 *A* and *B*). Notably, all peptides known to function as agonists contain an N-terminal carboxybenzyl group (29). The "reverse" binding orientation also explains why agonist peptides are not cleaved, because no peptide bond is positioned for nucleophilic attack by the active-site serine (Fig. 5). Nevertheless, agonist still would competitively inhibit binding of an actual substrate. Thus, agonist concentrations sufficient to bind many (but not all) of the 14 active sites can activate ClpP1P2 cleavage of peptide substrates, but very high agonist concentrations inhibit peptide cleavage (29).

ClpP1P2 variants with active-site mutations in one ring or the other have distinct substrate specificities, and the ClpP2 ring reacts preferentially with mechanism-based β-lactone inhibitors (29, 35). These observations can be explained by differences in the substrate-binding clefts of ClpP1 and ClpP2, which also affect Z-Ile-Leu binding. ClpP1 has a deep S1 pocket and a longer strand β9, which forms multiple hydrogen bonds with the backbone of the agonist peptide (Fig. 5*A* and Fig. S6*A*). In the structure, all Z-Ile-Leu molecules that bind to the active sites of ClpP1 adopted the same conformation with clear electron density for the entire peptide. In ClpP2, in contrast, a shallower S1 pocket and a shorter strand β9 terminated by a "bulge" (residues 139–143) resulted in a somewhat different Z-Ile-Leu conformation (Fig. 5*B* and Fig. S6*B*). For example, the bulge created a different binding site for the Ile side chain of the agonist, which packed against the side chain of Leu139. The electron density for Z-Ile-Leu molecules

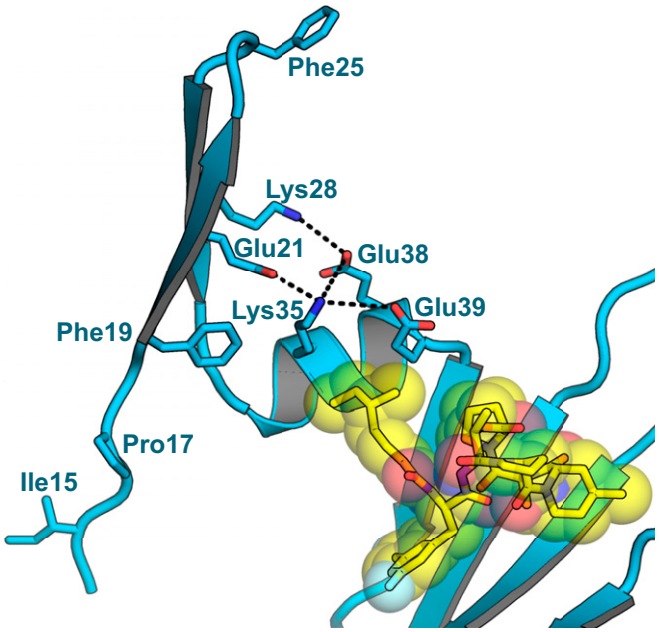

Fig. 4. The N-loops of ClpP2 (residues 19–30; cartoon and stick representation; cyan) adopt an extended β-hairpin that is stabilized by salt bridges (dashed lines) and packing between the acyl chain of an ADEP-2B^{5Me} molecule (stick and sphere representation; yellow) and the nonpolar portions of the Lys35 and Glu39 side chains.

bound to ClpP2 was strongest for the Z-Ile segment but was weaker at the C terminus (Fig. S1*E*), suggesting multiple conformations of the terminal Leu residue.

Interestingly, small channels were present near the active sites in the ClpP1 ring of ClpP1P2 (Figs. S5*A* and S7). In a few instances, electron density suggested that these channels were occupied partially by peptides, presumably additional molecules of Z-Ile-Leu. Although the large axial pores are likely to be the main conduits for substrate entry and product egress from the degradation chamber of ADEP-/agonist-stabilized ClpP1P2, the ClpP1 channels might play accessory roles in egress, especially in complexes of ClpP1P2 with ClpX and/or ClpC1.

Structural Basis of Homomeric-Ring Specificity and Heteromeric Tetradecamer Formation. Why are mixtures of ClpP1 and ClpP2 subunits not found in a single heptameric ring? Although many of the lateral interactions between subunits are similar in each ring, several unique interactions stabilize discrete ClpP1 or ClpP2 homoheptamers. In ClpP1, for example, the side chain of His117 forms salt bridges with the side chains of Asp79 and Glu149 in an adjacent ClpP1 subunit, as part of an extended polar network (Fig. 6*A*). ClpP2 lacks this histidine and cannot make analogous interactions with ClpP1. In ClpP2, the side chains of Tyr206, Arg207, and Lys208 in a structured C-terminal region make polar and packing interactions with residues in helix αC of an adjacent ClpP2 subunit (Fig. 6*B*). These residues are not conserved in ClpP1, and the corresponding C-terminal region of ClpP1 is disordered in both the ClpP1P2 and ClpP1P1 crystal structures.

In contrast, residues in the "handle" regions (αE and β9) that form the equatorial interface favor heteromeric association between a ClpP1 heptamer and a ClpP2 heptamer. In ClpP2, for example, the aromatic ring of Phe147, a residue located at the beginning of helix αE and the apex of the handle, projects into a hydrophobic pocket at the base of the ClpP1 handle, between αE and β9 (Fig. 6 *C* and *D*). Phe147 in ClpP2 is replaced by Ala133 in ClpP1. Thus, a homomeric ClpP1 tetradecamer would lack this stabilizing interaction. Although ClpP2 has a corresponding hydrophobic pocket at the base of its handle region, this pocket is unlikely to accommodate Phe147 from another ClpP2 ring, because modeling a ClpP2P2 tetradecamer based on ClpP1P2 predicted severe clashes between the two β9-bulge regions (Fig. S8). Rearranging these regions might permit interactions between ClpP2 rings but probably would collapse the adjacent substrate-binding pocket, distort the catalytic triad, and inactivate the enzyme.

Discussion

The ClpP1P2 structure provides a foundation for understanding the unusual properties of Clp-family proteases in *M. tuberculosis*. For example, the joint requirement of ClpP1 and ClpP2 for peptidase or protease activity (23, 29) is explained by the asymmetric but complementary equatorial interface between a ClpP1 heptamer and a ClpP2 heptamer in ClpP1P2. Symmetric interactions between either single ring are possible, as observed directly in the ClpP1P1 structure, but result in inactive tetradecamers with collapsed or occluded LGF-binding pockets and substrate-binding clefts.

This work provides insight into small-molecule stabilization of ClpP enzymes that do not form stable or active tetradecamers in isolation. Agonist and ADEP binding to ClpP1P2 were expected to mimic the binding of polypeptide substrates and AAA+ partners, respectively (14, 15, 20, 21, 23, 29). For both activating ligands, however, surprises emerged. For example, the Z-Ile-Leu agonist bound in a completely different orientation than an actual substrate. Despite this difference in orientation, agonists have activating effects similar to those of polypeptide substrates delivered by a AAA+ partner. In another surprise, ADEPs bound exclusively to the LGF-binding pockets of the ClpP2 ring but stabilized open axial pores and catalytically competent active-site conformations in both rings. Collectively, these observations

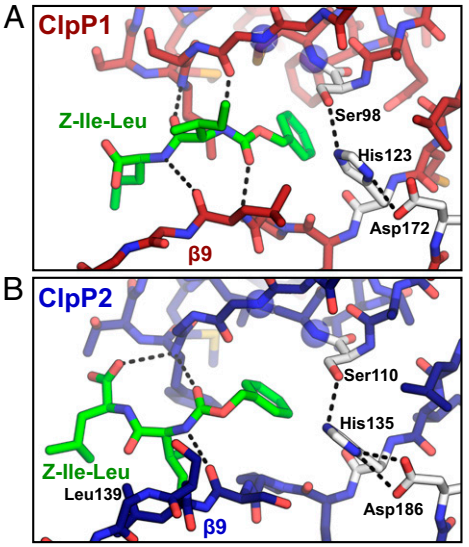

Fig. 5. Peptide agonists bind to the active sites of ClpP1 and ClpP2 in an orientation opposite that of peptide substrates. (*A*) Structure of the Z-Ile-Leu peptide (stick representation; green carbons) bound to the active site of ClpP1 (stick representation; most carbons are dark red; catalytic-triad carbons are white; small spheres mark oxyanion-hole NH groups). The N-terminal carboxybenzyl or Z blocking group occupies the S1 pocket, where the P1 residue of a substrate (on the C-terminal side of the scissile peptide bond) normally would bind. The backbone of the Z-Ile-Leu peptide forms a parallel β-sheet with strand β9, whereas a peptide substrate would bind in an antiparallel manner. (*B*) Binding of Z-Ile-Leu to the active site of ClpP2 (stick representation; most carbons are blue; catalytic-triad carbons are white; small spheres mark oxyanion-hole NH groups). A five-residue bulge, following a shorter β9, results in the side chains of the Z-Ile-Leu peptide making different interactions with ClpP2 than with ClpP1.

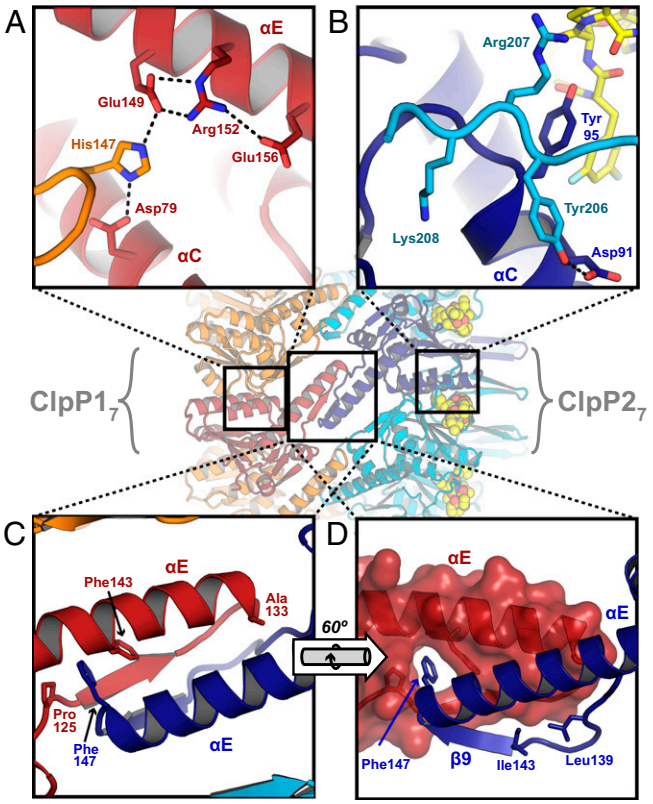

Fig. 6. Interactions that provide specificity within and between heptameric rings in ClpP1P2. (*A*) The side chain of His147 from one ClpP1 subunit (orange) is an integral part of a salt-bridge network that includes the side chains of Asp79, Glu149, Arg152, and Glu156 from a second ClpP1 subunit (red). (*B*) Residues 206–208 in the ordered C-terminal region of one ClpP2 subunit (cyan) interact with residues 91–95 in an adjacent ClpP2 subunit (blue). The side-chain hydroxyl of Tyr206 makes a hydrogen bond with Asp91; the aliphatic portion of the Arg207 side chain packs against the Tyr95 ring; and the side chain of Lys208 projects into a cleft with the side chain amine making a hydrogen bond with the carbonyl oxygen of Met93. (*C* and *D*) Asymmetric interface between the handle regions of ClpP1 (red and orange) and ClpP2 (blue and cyan). Phe147, at the tip of the ClpP2 handle, projects into a pocket at the base of the ClpP1 handle, whereas the symmetric Ala133 side chain in ClpP1 makes no comparable interaction. Strand β9 in ClpP2 is terminated by a bulge that projects inward and forms part of the substrate binding site (see Fig. 5*B*).

indicate that the conformations of the LGF-binding pockets, axial pores, and active sites in both rings of ClpP1P2 must be tightly and allosterically coupled. The synergy of ADEPs and agonists in activating ClpP1P2 indicates that both molecules bind preferentially to functional ClpP1P2 and thus stabilize this species relative to any inactive conformations.

There is substantial evidence that ADEP toxicity results from a gain-of-function mechanism in which the open axial pores of ADEP-bound ClpP allow entry and degradation of unfolded or misfolded proteins (14, 15, 20, 21). Because we find that ADEPs both open the pores and activate *M. tuberculosis* ClpP1P2, it is plausible that rogue degradation of cellular proteins is also responsible for ADEP killing of *M. tuberculosis* (30). However, given that the *M. tuberculosis clpX* and *clpC1* genes are essential (26–28), it also is possible that a loss-of-function mechanism contributes to ADEP killing. Specifically, ADEP disruption of the interaction between ClpP1P2 and an accessory AAA+ partner could lead to the accumulation of toxic proteins that are normally substrates of these Clp proteases (2). Indeed, in support of this possibility, our results clearly show that ADEPs inhibit protein degradation by ClpX•ClpP1P2.

An unusual feature of the ClpP1P2 system is the requirement for activators (23, 29). A mixture of ClpP1 and ClpP2 has very low peptidase activity and probably consists of a small concentration of active ClpP1P2 tetradecamers and much higher concentrations of numerous inactive species (heptamers of ClpP1 and ClpP2; tetradecamers of ClpP1P1, ClpP2P2, and possibly an inactive conformation of ClpP1P2). By binding more tightly to the subpopulation of active ClpP1P2 enzymes than to inactive molecules, ClpX, ClpC1, and the protein substrates they deliver shift the equilibrium toward this active species. This design couples ClpP1P2 activity to AAA+ partner activity, perhaps as a way to protect the cell from degradation by ClpP1P2 during periods of low metabolic activity when ATP and protein substrates are likely to be scarce (23).

The existence of discrete *M. tuberculosis* ClpP1 and ClpP2 rings might allow specialization compared with homomeric ClpPs, in which each ring normally can interact with several AAA+ partners (36). For example, structural differences between the LGF-binding pockets and N-loops of the ClpP1 and ClpP2 rings could result in ClpX binding to one ring and ClpC1 to the other ring, perhaps as a way to balance the degradation of substrates recognized by each AAA+ partner. Although the specificity of AAA+ partner binding to ClpP1P2 might be probed by mutating or perturbing one ring or the other, allosteric coupling complicates this approach. For instance, ADEP binds exclusively to the ClpP2 ring and inhibits ClpX•ClpP1P2 degradation, but this result could be explained by direct competition (ClpX binds ClpP2) and/or by an allosteric model (ClpX binds ClpP1). The detailed basis of heteromeric ClpP1P2 architecture reported here suggests an alternative approach for probing functional interactions with AAA+ partners, namely structure-based engineering of ClpP1 or ClpP2 variants in which mutations in the handle regions allow symmetric interfaces compatible with peptidase function and thus assembly of homomeric tetradecamers.

The ClpP1P2 structure and biochemical studies highlight the need for synergistic activation by two factors. For example, robust activation of ClpP1P2 in vitro requires a AAA+ partner and substrate delivery (23), a AAA+ partner and agonist peptide (29), or an ADEP and agonist peptide, as we have shown here. The assembly state of ClpP1P2 in vivo, and thus its sensitivity to hyperactivation and/or active-site inhibition, is not known. It seems likely, however, that physiological conditions that lead to very slow growth or metabolic inactivity also would render most ClpP1P2 resistant to inhibition or dysregulation. Under these conditions, a mixture of ADEPs and agonists could be more effective than ADEPs alone in killing *M. tuberculosis* and might sensitize the pathogen to killing by β-lactones (35) or other active-site inhibitors. The ClpP1P2 structure reported here also should aid in the design of new and more potent ADEPs and/or ADEP fragments that target both rings. Efforts toward this goal are underway.

Methods

Proteins and Small Molecules. Mature *M. tuberculosis* ClpP1 (residues 7–200) and ClpP2 (residues 13–214) with C-terminal His_6-tags were expressed and purified as described (35). For active-site labeling experiments, a SUMO domain was cloned between ClpP1 and the C-terminal His_6-tag, and the protein was purified in the same manner as ClpP1. For crystallography, ClpP1 labeled with selenomethionine was prepared by growing a strain containing a plasmid overexpressing ClpP1 in Luria–Bertani medium containing 100 mg/L L-selenomethionine for 5 h at room temperature and was purified as described (35). *M. tuberculosis* ClpX fused to an N-terminal His_7-SUMO domain to enhance solubility and H_6-GFP with a C-terminal ADSHQRDYALAA sequence corresponding to the *M. tuberculosis* ssrA tag (GFP-ssrA) were expressed and purified as described (23). ClpP concentrations are reported in tetradecamer equivalents. Z-Ile-Leu was purchased

from Sigma. Z-Leu-Leu-Nva-CHO was purchased from Boston Biochem. ADEPs and *N*-E-2-heptenoyldifluorophenylalanine methyl ester were synthesized as described (30, 31, 33, 37).

Enzymatic Assays. Assays were performed at 30 °C in a SpectraMax M5 microplate reader (Molecular Devices) in protein degradation (PD) buffer [25 mM Hepes, 100 mM KCl, 5 mM $MgCl_2$, 10% (vol/vol) glycerol, 5% (vol/vol) DMSO, 1 mM DTT, 0.1 mM EDTA, 0.1% Tween-20, pH 7.5]. Degradation of the fluorogenic Abz-KASPVSLGY^{NO2}D decapeptide (12) was followed by increases in fluorescence (excitation, 320 nm; emission, 420 nm). GFP-ssrA degradation was assayed by decreases in fluorescence (excitation, 380 nm; emission, 511 nm) in the presence of 2.5 mM ATP (Sigma) and a regeneration system consisting of 16 mM creatine phosphate (MP Biomedicals) and 0.32 mg/mL creatine phosphokinase (Sigma).

Active-Site Labeling. ClpP1P2 (0.5 μM) was incubated with TAMRA-fluorophosphonate (2 μM; Thermo Pierce) with or without ADEP-2B (50 μM) and/or Z-Ile-Leu (0.5 mM) in PD buffer at 30 °C. Reactions were quenched at different times by addition of SDS/PAGE loading buffer, frozen at –20 °C, and subjected to SDS/PAGE, and TAMRA fluorescence was detected using a Typhoon FLA 9500 imager (GE Healthcare Life Sciences).

Crystallization and Structure Determination. Hanging drops consisting of 0.6 μL protein [2.5 mg/mL selenomethionine-labeled ClpP1, 2.5 mg/mL ClpP2, 0.2 mM ADEP-2B^{5Me}, 0.5 mM Z-Ile-Leu, 10 mM Hepes, 50 mM NaCl, 0.5 mM TCEP, 15% (vol/vol) DMSO, pH 7.5] and 0.6 μL precipitant [1.5 M $(NH_4)_2SO_4$, 0.1 M MES, pH 6.5] were suspended over a reservoir of 500 μL of precipitant and incubated at 20 °C. Rod-shaped hexagonal crystals (50 × 50 × 200 μm) and rectangular crystals (100 × 100 × 200 μm) formed over a period of ∼9 mo. Crystals were soaked briefly in cryoprotection solution (1.9 M Li_2SO_4, 50 mM MES, pH 6.5) and flash frozen in liquid N_2.

X-ray diffraction data were collected at the Advanced Photon Source (APS) beamlines 24-ID-C (ClpP1P1) and 24-ID-E (ClpP1P2) at 100 K and with X-ray wavelengths near the Se edge (0.9790 Å for ClpP1P1; 0.9792 Å for ClpP1P2). Raw data were processed using HKL2000 (38). The ClpP1P1 structure was solved by molecular replacement with Phaser (39) as implemented in CCP4 (40) using the ClpP1 structure [Protein Data Bank (PDB) ID code 2CE3] as a search model (32). The ClpP1P2 structure was solved by molecular replacement using search models for a ClpP1 heptamer (PDB ID code 2CE3) (32) and a ClpP2 heptamer model based on *E. coli* ClpP (PDB ID code 1TYF) (9). Models were built with Coot (41) and refined using Phenix (42), with torsion-based noncrystallographic restraints for identical chains in the asymmetric unit. The percentage of residues with favored/allowed/disallowed Ramachandran dihedral angles was 97.7/2.3/0 for the ClpP1P1 structure and 98.6/1.4/0 for the ClpP1P2 structure. Coordinates for both structures have been deposited in the Protein Data Bank with ID codes 4U0G (ClpP1P2) and 4U0H (ClpP1).

ACKNOWLEDGMENTS. We thank D. Dowling and M. Funk for crystallographic data collection and A. Amor, C. Compton, B. Hall, A. Olivares, and B. Stinson for helpful discussions. This work was supported by National Institutes of Health (NIH) Grant GM-101988 and funding from Brown University. J.K.S. was supported by a National Science Foundation CAREER Award. Studies at the North East Collaborative Access Team beamlines of the Advanced Photon Source were supported by the NIH National Institute of General Medical Sciences Grant P41 GM103403 and the US Department of Energy under Contract DE-AC02-06CH11357.

1. Yu AYH, Houry WA (2007) ClpP: A distinctive family of cylindrical energy-dependent serine proteases. *FEBS Lett* 581(19):3749–3757.
2. Aakre CD, Phung TN, Huang D, Laub MT (2013) A bacterial toxin inhibits DNA replication elongation through a direct interaction with the β sliding clamp. *Mol Cell* 52(5):617–628.
3. Gispert S, et al. (2013) Loss of mitochondrial peptidase Clpp leads to infertility, hearing loss plus growth retardation via accumulation of CLPX, mtDNA and inflammatory factors. *Hum Mol Genet* 22(24):4871–4887.
4. Gaillot O, Pellegrini E, Bregenholt S, Nair S, Berche P (2000) The ClpP serine protease is essential for the intracellular parasitism and virulence of *Listeria monocytogenes*. *Mol Microbiol* 35(6):1286–1294.
5. Kwon HY, et al. (2004) The ClpP protease of *Streptococcus pneumoniae* modulates virulence gene expression and protects against fatal pneumococcal challenge. *Infect Immun* 72(10):5646–5653.
6. Loughlin MF, Arandhara V, Okolie C, Aldsworth TG, Jenks PJ (2009) *Helicobacter pylori* mutants defective in the clpP ATP-dependant protease and the chaperone clpA display reduced macrophage and murine survival. *Microb Pathog* 46(1):53–57.
7. Li Y, et al. (2010) ClpXP protease regulates the type III secretion system of *Dickeya dadantii* 3937 and is essential for the bacterial virulence. *Mol Plant Microbe Interact* 23(7):871–878.
8. Li XH, et al. (2010) The ClpP protease homologue is required for the transmission traits and cell division of the pathogen *Legionella pneumophila*. *BMC Microbiol* 10:54.
9. Wang J, Hartling JA, Flanagan JM (1997) The structure of ClpP at 2.3 A resolution suggests a model for ATP-dependent proteolysis. *Cell* 91(4):447–456.
10. Alexopoulos JA, Guarné A, Ortega J (2012) ClpP: A structurally dynamic protease regulated by AAA+ proteins. *J Struct Biol* 179(2):202–210.
11. Thompson MW, Maurizi MR (1994) Activity and specificity of *Escherichia coli* ClpAP protease in cleaving model peptide substrates. *J Biol Chem* 269(27):18201–18208.
12. Lee ME, Baker TA, Sauer RT (2010) Control of substrate gating and translocation into ClpP by channel residues and ClpX binding. *J Mol Biol* 399(5):707–718.
13. Sauer RT, Baker TA (2011) AAA+ proteases: ATP-fueled machines of protein destruction. *Annu Rev Biochem* 80:587–612.
14. Lee BG, et al. (2010) Structures of ClpP in complex with acyldepsipeptide antibiotics reveal its activation mechanism. *Nat Struct Mol Biol* 17(4):471–478.
15. Li DH, et al. (2010) Acyldepsipeptide antibiotics induce the formation of a structured axial channel in ClpP: A model for the ClpX/ClpA-bound state of ClpP. *Chem Biol* 17(9):959–969.
16. Kim YI, et al. (2001) Molecular determinants of complex formation between Clp/Hsp100 ATPases and the ClpP peptidase. *Nat Struct Biol* 8(3):230–233.
17. Singh SK, et al. (2001) Functional domains of the ClpA and ClpX molecular chaperones identified by limited proteolysis and deletion analysis. *J Biol Chem* 276(31):29420–29429.
18. Joshi SA, Hersch GL, Baker TA, Sauer RT (2004) Communication between ClpX and ClpP during substrate processing and degradation. *Nat Struct Mol Biol* 11(5):404–411.
19. Martin A, Baker TA, Sauer RT (2007) Distinct static and dynamic interactions control ATPase-peptidase communication in a AAA+ protease. *Mol Cell* 27(1):41–52.
20. Brötz-Oesterhelt H, et al. (2005) Dysregulation of bacterial proteolytic machinery by a new class of antibiotics. *Nat Med* 11(10):1082–1087.
21. Kirstein J, et al. (2009) The antibiotic ADEP reprogrammes ClpP, switching it from a regulated to an uncontrolled protease. *EMBO Mol Med* 1(1):37–49.
22. Gominet M, Seghezzi N, Mazodier P (2011) Acyl depsipeptide (ADEP) resistance in Streptomyces. *Microbiology* 157(Pt 8):2226–2234.
23. Schmitz KR, Sauer RT (2014) Substrate delivery by the AAA+ ClpX and ClpC1 unfoldases activates the mycobacterial ClpP1P2 peptidase. *Mol Microbiol* 93(4):617–628.
24. Personne Y, Brown AC, Schuessler DL, Parish T (2013) *Mycobacterium tuberculosis* ClpP proteases are co-transcribed but exhibit different substrate specificities. *PLoS ONE* 8(4):e60228.
25. Sherrid AM, Rustad TR, Cangelosi GA, Sherman DR (2010) Characterization of a Clp protease gene regulator and the reaeration response in *Mycobacterium tuberculosis*. *PLoS ONE* 5(7):e11622.
26. Sassetti CM, Boyd DH, Rubin EJ (2003) Genes required for mycobacterial growth defined by high density mutagenesis. *Mol Microbiol* 48(1):77–84.
27. Griffin JE, et al. (2011) High-resolution phenotypic profiling defines genes essential for mycobacterial growth and cholesterol catabolism. *PLoS Pathog* 7(9):e1002251.
28. Raju RM, et al. (2012) *Mycobacterium tuberculosis* ClpP1 and ClpP2 function together in protein degradation and are required for viability *in vitro* and during infection. *PLoS Pathog* 8(2):e1002511.
29. Akopian T, et al. (2012) The active ClpP protease from *M. tuberculosis* is a complex composed of a heptameric ClpP1 and a ClpP2 ring. *EMBO J* 31(6):1529–1541.
30. Ollinger J, O'Malley T, Kesicki EA, Odingo J, Parish T (2012) Validation of the essential ClpP protease in *Mycobacterium tuberculosis* as a novel drug target. *J Bacteriol* 194(3):663–668.
31. Carney DW, Schmitz KR, Truong JV, Sauer RT, Sello JK (2014) Restriction of the conformational dynamics of the cyclic acyldepsipeptide antibiotics improves their antibacterial activity. *J Am Chem Soc* 136(5):1922–1929.
32. Ingvarsson H, et al. (2007) Insights into the inter-ring plasticity of caseinolytic proteases from the X-ray structure of *Mycobacterium tuberculosis* ClpP1. *Acta Crystallogr D Biol Crystallogr* 63(Pt 2):249–259.
33. Carney DW, et al. (2014) A simple fragment of cyclic acyldepsipeptides is necessary and sufficient for ClpP activation and antibacterial activity. *ChemBioChem*, 10.1002/cbic.201402358.
34. Szyk A, Maurizi MR (2006) Crystal structure at 1.9A of *E. coli* ClpP with a peptide covalently bound at the active site. *J Struct Biol* 156(1):165–174.
35. Compton CL, Schmitz KR, Sauer RT, Sello JK (2013) Antibacterial activity of and resistance to small molecule inhibitors of the ClpP peptidase. *ACS Chem Biol* 8(12):2669–2677.

36. Grimaud R, Kessel M, Beuron F, Steven AC, Maurizi MR (1998) Enzymatic and structural similarities between the *Escherichia coli* ATP-dependent proteases, ClpXP and ClpAP. *J Biol Chem* 273(20):12476–12481.
37. Hinzen B, et al. (2006) Medicinal chemistry optimization of acyldepsipeptides of the enopeptin class antibiotics. *ChemMedChem* 1(7):689–693.
38. Otwinowski Z, Minor W (1997) Processing of X-ray Diffraction Data Collected in Oscillation Mode. *Macromolecular Crystallography*, eds Carter, Jr CW, Sweet RM (Academic, New York), pp 307–326.
39. McCoy AJ, et al. (2007) Phaser crystallographic software. *J Appl Cryst* 40(Pt 4):658–674.
40. Collaborative Computational Project, Number 4 (1994) The CCP4 suite: Programs for protein crystallography. *Acta Crystallogr D Biol Crystallogr* 50(Pt 5):760–763.
41. Emsley P, Cowtan K (2004) Coot: Model-building tools for molecular graphics. *Acta Crystallogr D Biol Crystallogr* 60(Pt 12 Pt 1):2126–2132.
42. Adams PD, et al. (2010) PHENIX: A comprehensive Python-based system for macromolecular structure solution. *Acta Crystallogr D Biol Crystallogr* 66(Pt 2): 213–221.